Sensitive Electric Field Measurement by Fluorescence-Dip Spectroscopy of Rydberg States of Atomic Hydrogen

U. Czarnetzki,* D. Luggenhölscher, and H. F. Döbele

Institut für Laser- und Plasmaphysik, Universität GH Essen, 45117 Essen, Germany

(Received 27 July 1998)

Fluorescence-dip spectroscopy based on an optical double resonance is used to probe the Stark splitting in highly excited Rydberg states of atomic hydrogen. After Doppler-free two-photon excitation to $n = 3$, fluorescence at Balmer α is observed. When the radiation of a second laser is tuned over the resonance between $n = 3$ and a Rydberg state, the Stark splitting manifests itself as a series of dips in the Balmer-α fluorescence intensity. Rydberg states up to $n = 55$ can be identified. The minimum detectable electric field is 5 V/cm. This is about an order of magnitude more sensitive than other laser-induced fluorescence techniques. [S0031-9007(98)07702-3]

PACS numbers: 32.60.+i

There has been a growing interest in recent years in the diagnostics of sheath phenomena in dc and rf discharges by electric field measurements based on laser spectroscopy. Several spectroscopic methods have been developed [1–6]. These methods are based on the measurement of the Stark splitting or state mixing of Rydberg states in various media, such as diatomic molecules, noble gases, and atomic hydrogen. An alternative method based on a coherent anti-Stokes Raman scattering scheme has also been described recently [7]. By the detection of an optogalvanic signal highly excited Rydberg states in helium could be probed. This technique, however, is not feasible in high frequency discharges. Methods based on laser-induced fluorescence spectroscopy (LIF) are limited by the long lifetime and unfavorable branching ratio of the Rydberg states. In atomic hydrogen the highest Rydberg state that could be probed by LIF is $n = 6$ [6]. In this paper we describe a novel LIF technique for electric field measurement based on an optical double resonance that overcomes the limitations by long lifetimes and allows the measurement of the Stark splitting of highly excited Rydberg states in atomic hydrogen.

The general scheme is similar to that first introduced by Ebata *et al.* in 1983 for the investigation of highly excited states in NO [8]. Here the scheme is applied to atomic hydrogen (Fig. 1). Hydrogen atoms are excited in a first step by Doppler-free two-photon absorption from the ground state to $n = 3$ by UV radiation at $\lambda = 205$ nm. Fluorescence at the Balmer-α line ($\lambda = 656$ nm) is observed subsequently. The Doppler-free two-photon step has the advantage that focusing can be avoided and that therefore two-dimensional spatially resolved measurements are possible by transverse imaging. In addition, the laser intensity can be kept at a low level so that ionization of atoms by a third UV photon and dissociation of molecules of the background gas are greatly avoided.

The radiation of a second laser in the near IR is tuned over the Stark-split resonance between $n = 3$ and a Rydberg state. If the IR radiation is resonant, population is transferred from $n = 3$ to the Rydberg state, and the fluorescence intensity at Balmer alpha is consequently decreased. The fluorescence intensity therefore exhibits a series of dips as a function of the IR wavelength which represent the Stark spectrum of the respective Rydberg state.

The dip spectra are insensitive to the lifetime of the Rydberg state so that almost any Rydberg state can be probed. A practical limit is given by the laser energy necessary to transfer a sufficient amount of population to the Rydberg state within the short pulse width of the laser. With increasing principal quantum number an accordingly higher energy is necessary. A simple rate equation calculation shows that the product of the two-level saturation parameter with the Einstein coefficient for spontaneous emission and the laser pulse width should be of the order or larger than 1. Depending on the Rydberg state, the required energy can range from a few μJ to several mJ.

The electric field strength is deduced by comparing measured and calculated spectra. The resulting dip spectra are determined by both the Stark effect of the initial $n = 3$ and the final Rydberg states. The Stark splitting in

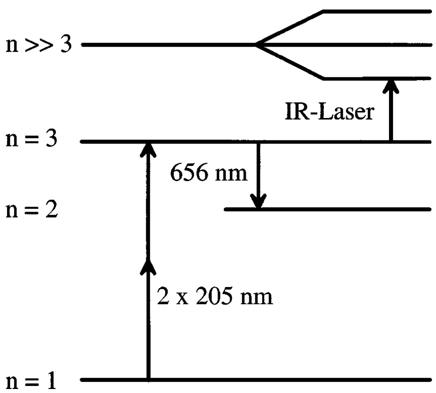

FIG. 1. Scheme for fluorescence-dip spectroscopy in atomic hydrogen.

$n = 3$ is small compared to that of the Rydberg state and is not observed in the measured spectra, but the mixing of the five fine-structure components in $n = 3$ has a strong effect on the shape of the spectrum. In addition, the relative matrix elements for the two-photon excitation process from the ground state to $n = 3$ have to be taken into account. Theoretical spectra are calculated in the following way: For a given electric field the new eigenvectors and eigenvalues in $n = 3$ and in the Rydberg state are calculated by standard perturbation theory [9–11]. The relative absorption line strengths for the allowed transitions between these new states and the respective transition frequencies are then calculated. Each transition is further multiplied by a weight factor for the relative population of the lower state after two-photon excitation. This factor depends on the mixing of the states in $n = 3$ and takes account also of the spectral two-photon excitation profile. Matrix elements are taken from Refs. [12,13]. Finally, the spectrum is convoluted by the absorption profile. Both spectral profiles are determined experimentally at zero field.

Spectra calculated for $n = 14$ are shown in Fig. 2. In this figure as well as in the following figures showing measurements, the spectra are inverted so that the dips appear as peaks. The calculations were performed with a UV-laser linewidth of 0.14 cm^{-1}, a Doppler width of 1.2 cm^{-1} ($T = 300$ K), and an absorption linewidth of 0.5 cm^{-1}. Both lasers are polarized parallel to the electric field.

A remarkable feature of the spectrum is the absence of a central peak. With the polarization of the IR-laser radiation perpendicular to the field, however, a strong central line appears. This is true for all even principal quantum numbers. The situation is reversed in the case of odd quantum numbers. Provided the individual Stark components are sufficiently well resolved, the direction of the field can therefore be determined from the intensity of the central component. However, the spectra do not depend on the sign of the electric field.

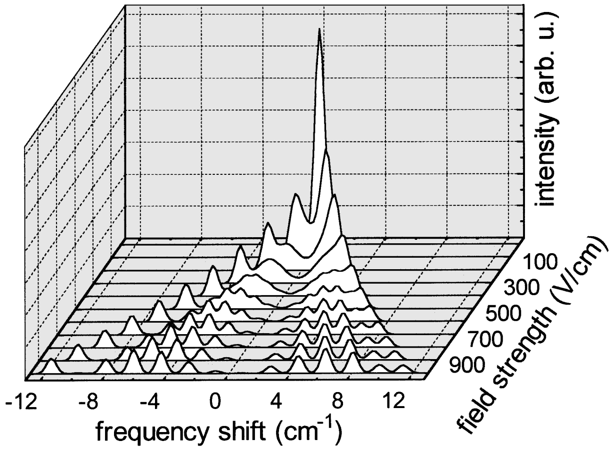

FIG. 2. Theoretical Stark spectrum for $n = 14$. The UV and IR laser fields are both polarized parallel to the electric field.

Experiments are performed in atomic hydrogen generated by the aid of a flow tube reactor [14] and in a capacitively coupled rf discharge. The flow tube reactor allows measurements under well defined external fields and the rf discharge measurements are performed in order to demonstrate the applicability of the novel technique to gas discharges. Part of the experiment is described in more detail in [15]. The discharge chamber is the Gaseous Electronics Conference (GEC) reference cell [16]. The GEC cell consists of two parallel electrodes, 10 cm in diameter and separated by 2.5 cm. The rf discharge is operated in pure hydrogen at a pressure of 80 Pa. Electric fields are measured in the sheath region in front of the powered electrode.

The flow tube reactor is mounted to the GEC cell with the rf discharge switched off. Atomic hydrogen is generated in an external microwave discharge and guided by a Teflon tube to the region between the electrodes. A low dc voltage is applied to the electrodes and a well defined homogeneous electric field is therefore established. The maximum voltage that can be applied before a discharge ignites is about 250 V, corresponding to a maximum electric field of 100 V/cm. Typical atomic hydrogen densities in both the flow tube reactor and the rf discharge are of the order of a few 10^{20} m^{-3}.

The laser system consists of two Nd:YAG-pumped dye lasers (Continuum Powerlite 8010 and ND6000) with one dye laser equipped with frequency doubling and mixing in a beta-barium borate (BBO) crystal. About 3 mJ in 3 ns pulses are generated at a bandwidth of 0.14 cm^{-1}. The second dye laser is followed by a high pressure H_2-Raman cell. It generates several mJ of tunable IR radiation with a pulse width of about 4 ns and a bandwidth of 0.1 cm^{-1}. With a single mixture of dyes (DCM, Rhodamine-B) the system is continuously tunable between 820 and 925 nm, allowing the excitation of Rydberg states between $n = 9$ and the ionization limit. The UV laser passes through the center of the GEC cell. Doppler-free excitation is realized by a mirror close to the exit window that reflects the beam back into itself. The IR laser beam is transmitted by this mirror and is adjusted collinear to the UV beam.

The fluorescence light at Balmer-α ($\lambda = 656$ nm) is imaged perpendicular to the laser beams onto a gated intensified charge-coupled device (ICCD) camera (Princeton Instruments) with a high and a low pass filter in front. Light from several laser shots (typical 150) is accumulated on the camera. The laser pulses are locked to a certain phase within the rf cycle and the ICCD-camera gate is adjusted accordingly.

Figure 3 shows a scan of the IR laser wavelength at zero field. The atomic hydrogen is generated by the flow tube reactor. The electrodes are short circuited and grounded in order to avoid possible autocharging effects. Resonances of Rydberg states up to $n = 55$ can be observed. Spectra and full widths at half maximum (FWHM) deduced from these spectra with the laser tuned to $n = 30$ at various applied electric field strengths are

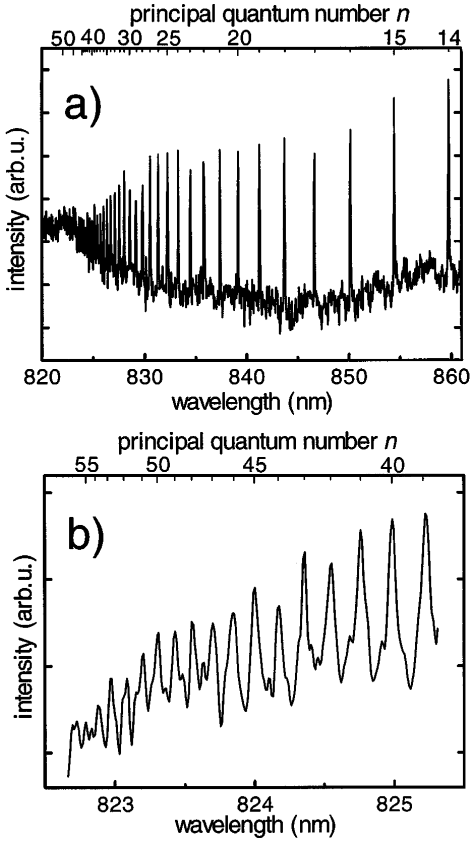

FIG. 3. Scan of the IR laser wavelength over Rydberg state resonances at zero field.

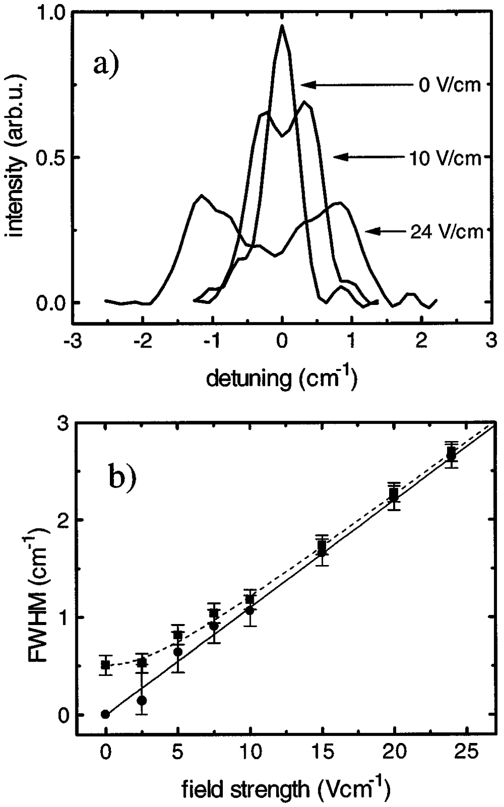

FIG. 4. (a) Measured spectra with $n = 30$ at various field strengths. (b) Measured FWHM (squares) and reduced FWHM (circles) after deconvolution. The solid line is the theoretical curve.

shown in Fig. 4. The reduced half-widths are obtained after deconvolution with the profile measured at zero field. Saturation broadening accounts for the most of the linewidth of this profile $(\sim\frac{2}{3})$. The slope of the resulting linear field dependence corresponds very well to the theoretical curve. The minimum electric field that can be measured reliably is about 5 V/cm.

The measured slopes of various Rydberg states are shown in Fig. 5. The slope is a measure of the field sensitivity of the Stark splitting. The measurement error is of the order of the size of the data points. The data points fit very well the theoretically expected increase by $n(n-1)(1.28 \times 10^{-4}\ V^{-1})$. The deviation of the slope for $n = 40$ from this line is surprising. One possible explanation could be that the neighboring Rydberg states are already mixed to $n = 40$ and that therefore the simple rule $\propto n(n-1)$ does no more apply exactly.

Figure 5 also shows the maximum field strength that can be measured before the Stark spectrum of one Rydberg state starts to overlap with the spectrum of the next higher state. The spectral distance between two neighboring states scales as n^{-3}. For reliable electric field measurements the distance to the next higher Rydberg state should at least be a few times the zero field linewidth, e.g., 4 times. We find experimentally a typical linewidth of about 0.7 ± 0.2 cm^{-1}, almost independent of the Rydberg state. The highest Rydberg state that can be used for electric field measurements under these experimental conditions is therefore $n = 43$. Compared with $n = 30$ we could not measure a significantly lower electric field by going to $n = 40$ due to the lower signal

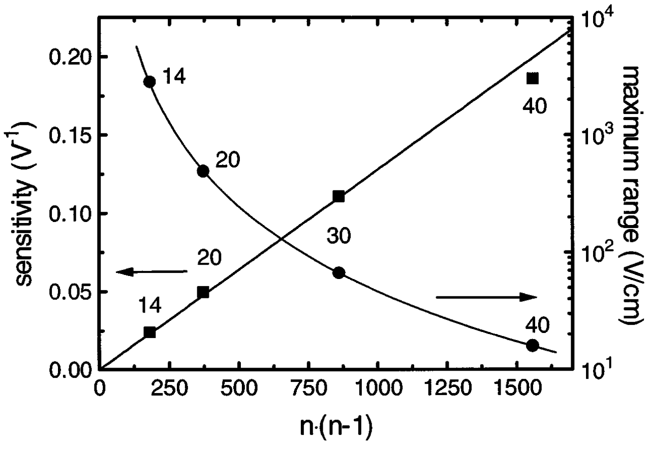

FIG. 5. Left scale (squares): Measured sensitivities (spectral shift of the outermost Stark components per unit electric field) as a function of the principal quantum number n of the Rydberg states. The solid line represents the theoretical $n(n-1)$ dependence. Right scale (circles): Calculated maximum electric field strength that can be measured without overlap of neighboring spectra. At each data point the according principal quantum number is indicated.

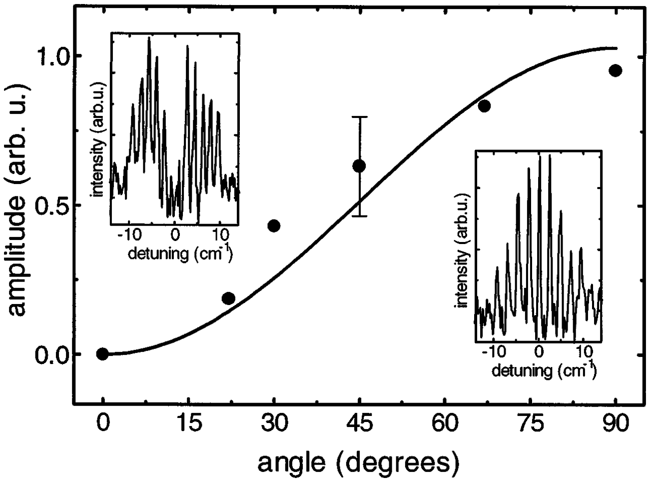

FIG. 6. Relative amplitude of the central peak of the Stark spectrum of $n = 14$ as a function of the angle between the polarization of the IR laser beam and the electric field. The field strength is 950 V/cm. Typical spectra with the polarization parallel (left) and perpendicular (right) to the field are shown in the insets.

amplitude and the accordingly lower signal-to-noise-ratio. Our low field limit is therefore 5 V/cm. This is about an order of magnitude more sensitive than other LIF techniques.

The polarization dependence was verified in the rf discharge (Fig. 6). The insets show typical spectra of the Stark splitting for $n = 14$ at fields of 950 V/cm with the polarization of the IR laser beam parallel and perpendicular to the field. The relative intensity of the central peak is plotted in the main figure as a function of the polarization angle ϕ of the IR laser beam with respect to the electric field. The solid line in Fig. 6 shows the expected $\sin(\phi)^2$ dependence. This measurement demonstrates the applicability of the fluorescence-dip technique to plasma discharges.

We find $n = 14$ a particularly well suited Rydberg state for applications to electric field measurements in the sheath region of rf and dc discharges since the spectrum has a high amplitude and allows a large dynamic range with a minimum electric field of about 25 V/cm and a maximum field of about 2600 V/cm. It covers therefore the entire range of field strengths typical for the sheath region in these discharges. Application to discharges in, e.g., methane or silane which contain a large amount of atomic hydrogen should be straightforward. The fluorescence-dip spectroscopy scheme can in principle also be applied to other atomic systems which exhibit two-photon resonances in the UV, e.g., nitrogen, oxygen, or chlorine. This would allow the investigation of a large number of discharges with technological importance. The Stark effect in the Rydberg states of these atoms will probably be more complex than in hydrogen and a calibration measurement will be necessary. Such a calibration measurement has been demonstrated recently in [17] by the comparison between the complex Stark spectra in argon with the well understood spectra in helium.

This project is supported by the “Bundesminister für Bildung und Forschung.” Expert technical assistance by Rainer Führer is gratefully acknowledged.

---

*Author to whom correspondence should be addressed. Email address: uwe.czarnetzki@uni-essen.de

[1] R. A. Gottscho, Phys. Rev. A **36**, 2233 (1987).
[2] J. E. Lawler and D. A. Doughty, Adv. At. Mol. Opt. Phys. **34**, 171 (1994).
[3] B. N. Ganguly, J. Appl. Phys. **60**, 571 (1986).
[4] M. P. Alberta, H. Debontride, J. Derouard, and N. Sadeghi, J. Phys. III (France) **3**, 105 (1993).
[5] G. A. Hebner, K. Greenberg, and M. E. Riley, J. Appl. Phys. **76**, 4036 (1994).
[6] J. P. Booth, M. Fadlallah, J. Derouard, and N. Sadeghi, Appl. Phys. Lett. **65**, 819 (1994).
[7] V. N. Ochkin, S. Yu. Savinov, S. N. Tskhai, U. Czarnetzki, V. Schulz-von der Gathen, and H. F. Döbele, IEEE Trans. Plasma Sci. (to be published).
[8] T. Ebata, N. Mikami, and M. Ito, J. Chem. Phys. **78**, 1132 (1983).
[9] Hans A. Bethe and Edwin E. Salpeter, *Quantum Mechanics of One- and Two-Electron Atoms* (Plenum Publishing Corporation, New York, 1977).
[10] Igor I. Sobelman, *Atomic Spectra and Radiative Transitions* (Springer-Verlag, Heidelberg, 1979).
[11] Robert D. Cowan, *The Theory of Atomic Structure and Spectra* (University of California Press, Berkeley, 1981).
[12] J. E. M. Goldsmith and L. A. Rahn, Opt. Lett. **15**, 814 (1990).
[13] Majida Fadlallah, doctoral thesis, Université Joseph Fourier–Grenoble I, 1995.
[14] D. W. Setser, *Reactive Intermediates in the Gas Phase* (Academic Press, New York, 1979).
[15] L. Cherigier, U. Czarnetzki, D. Luggenhölscher, V. Schulz-von der Gathen, and H. F. Döbele, J. Appl. Phys. (to be published).
[16] P. J. Hargis *et al.*, Rev. Sci. Instrum. **65**, 140 (1994).
[17] J. B. Kim, K. Kawamura, Y. W. Choi, M. D. Bowden, K. Muraoka, and V. Helbig, IEEE Trans. Plasma Sci. (to be published).